

Role of Septin Cytoskeleton in Spine Morphogenesis and Dendrite Development in Neurons

Tomoko Tada, Alyson Simonetta, Matthew Batterton,
Makoto Kinoshita, Dieter Edbauer, and Morgan Sheng

Supplemental References

- S1. Dunah, A.W., Hueske, E., Wyszynski, M., Hoogenraad, C.C., Jaworski, J., Pak, D.T., Simonetta, A., Liu, G., and Sheng, M. (2005). LAR receptor protein tyrosine phosphatases in the development and maintenance of excitatory synapses. *Nat. Neurosci.* 8, 458–467.
- S2. Jaworski, J., Spangler, S., Seeburg, D.P., Hoogenraad, C.C., and Sheng, M. (2005). Control of dendritic arborization by the phosphoinositide-3'-kinase-Akt-mammalian target of rapamycin pathway. *J. Neurosci.* 25, 11300–11312.
- S3. Hoogenraad, C.C., Milstein, A.D., Ethell, I.M., Henkemeyer, M., and Sheng, M. (2005). GRIP1 controls dendrite morphogenesis by regulating EphB receptor trafficking. *Nat. Neurosci.* 8, 906–915.
- S4. Kinoshita, M., Field, C.M., Coughlin, M.L., Straight, A.F., and Mitchison, T.J. (2002). Self- and actin-templated assembly of Mammalian septins. *Dev. Cell* 3, 791–802.
- S5. Ihara, M., Kinoshita, A., Yamada, S., Tanaka, H., Tanigaki, A., Kitano, A., Goto, M., Okubo, K., Nishiyama, H., Ogawa, O., et al. (2005). Cortical organization by the septin cytoskeleton is essential for structural and mechanical integrity of mammalian spermatozoa. *Dev. Cell* 8, 343–352.
- S6. Kinoshita, A., Noda, M., and Kinoshita, M. (2000). Differential localization of septins in the mouse brain. *J. Comp. Neurol.* 428, 223–239.

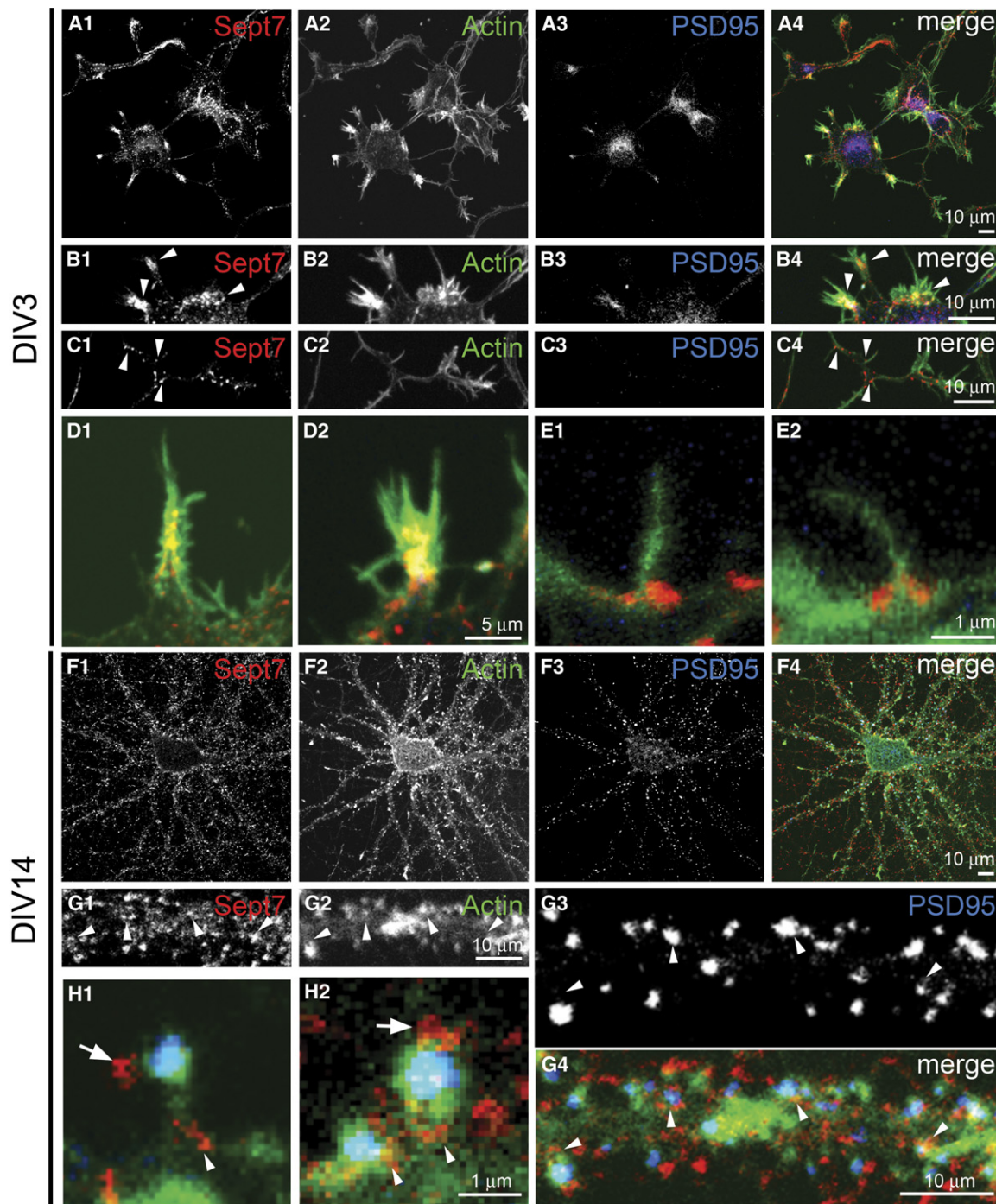


Figure S1. Localization of Endogenous Sept7 in Cultured Hippocampal Neurons at DIV3 and DIV14

Neurons were fixed and immunostained for Sept7 (red), F-actin (phalloidin staining, green), and PSD-95 (blue) at DIV3 (A–E) and at DIV14 (F–H). Shown in (A) are low-magnification images of whole neurons (DIV3). Shown in (B) is Sept7 at the base of actin-rich growth cones emerging from the cell soma (arrowheads). As shown in (C), Arrowheads indicate Sept7 at the base of small branches from the presumptive axon. Shown in (D) are merged images (Sept7 red; actin, green) of individual growth cones at high magnification. Shown in (E) are merged images of axonal branches at high magnification. Shown in (F) are low-magnification images of neurons at DIV14 stained for Sept7, F-actin, and PSD-95. Shown in (G) are higher-magnification images of dendrite segments. Arrowheads indicate Sept7 at the base of actin-rich dendritic protrusions. Shown in (H) are individual dendritic protrusions at high magnification. Arrowheads indicate Sept7 (red) localized at the base of protrusions containing PSD-95 (blue). Arrows indicate Sept7 clusters (red) apposed to the outside of dendritic protrusions—presumably presynaptically localized Sept7.

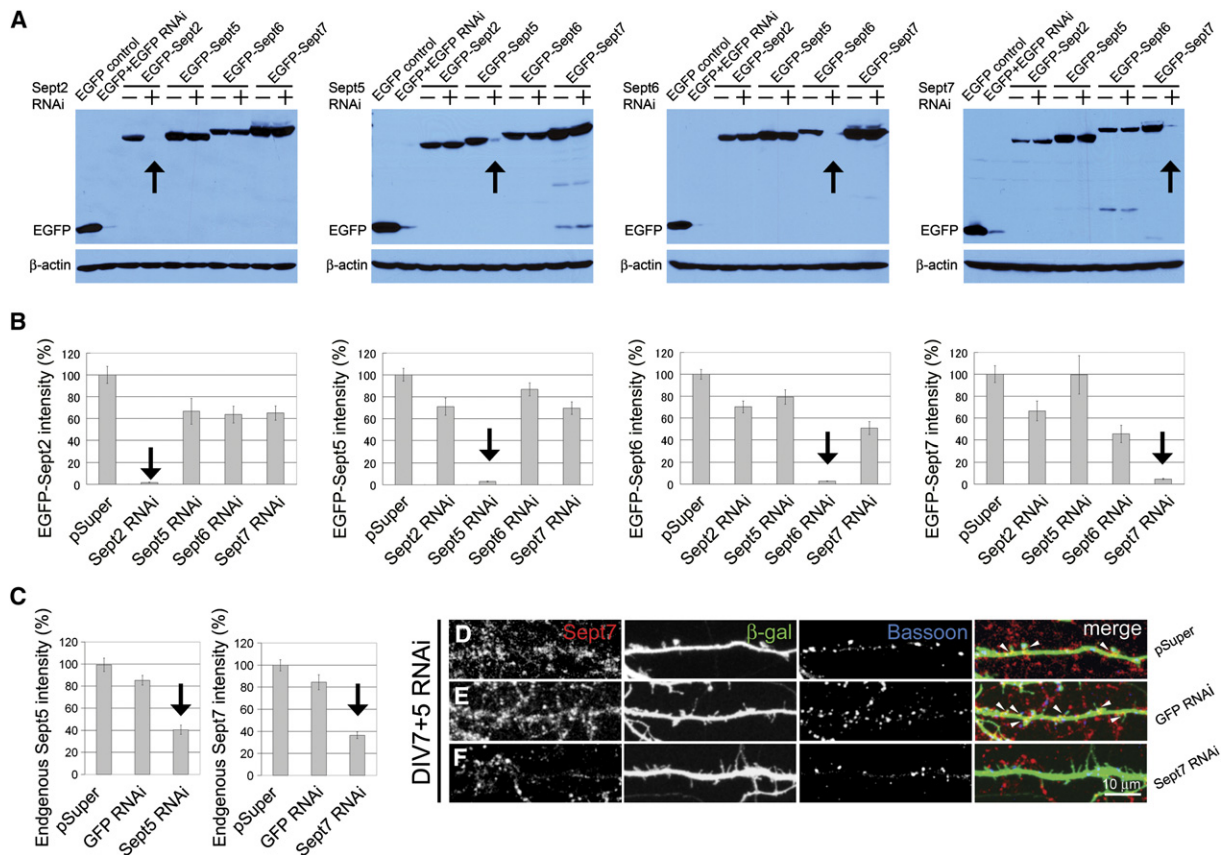


Figure S2. Specific Knockdown of Septins by RNAi

(A) HEK293 cells were transfected with EGFP-Sept2, -Sept5, -Sept6, or -Sept7 as indicated, together with pSuper vector control (–) or with pSuper-based RNAi constructs designed to knockdown the specific septin indicated (+). Two days after transfection, EGFP-Septin levels were analyzed by immunoblotting with an anti-EGFP antibody. Each RNAi construct specifically knocks down the corresponding septin (arrows) without affecting expression of other septin family members. EGFP targeted by EGFP-RNAi served as the positive control (right two lanes).

(B) To test specific knockdown in neurons, we cotransfected EGFP-Sept2, -Sept5, -Sept6, or -Sept7 together with various RNAi constructs targeting different septins into neurons and quantified the EGFP-Septin fluorescence intensity at 5 days after transfection (DIV7+5). Arrows show that each RNAi knocks down the corresponding septin. $n > 25$ cells for each histogram.

(C) Cultured hippocampal neurons (DIV7) were transfected with empty vector pSuper or EGFP RNAi, Sept5 RNAi, or Sept7 RNAi constructs, as indicated. At 5 days after transfection (DIV7+5), endogenous Sept5 or Sept7 were immunostained by specific antibody, and transfected neurons were identified by immunostaining for cotransfected β -gal. Endogenous Sept5 and Sept7 immunofluorescence intensity was specifically reduced by Sept5-RNAi (left panel) and Sept7-RNAi constructs (right panel). “n” numbers for each condition were pSuper (23), EGFP-RNAi (37), and Sept5-RNAi (25), for immunostaining with the Sept5 antibody. “n” numbers for each condition were pSuper (88), EGFP-RNAi (25), and Sept7-RNAi (73), for immunostaining with the Sept7 antibody. Arrows show that each RNAi knocks down the corresponding septin.

(D–F) Representative dendrites of neurons (DIV7+5) transfected with pSuper (D), EGFP RNAi (E), or Sept7 RNAi (F) and triple labeled for Sept7 (red), β -gal (green), and Bassoon (blue), as indicated. Arrowheads show that endogenous Sept7 are localized at the base of dendritic protrusions. All histograms show mean \pm SEM.

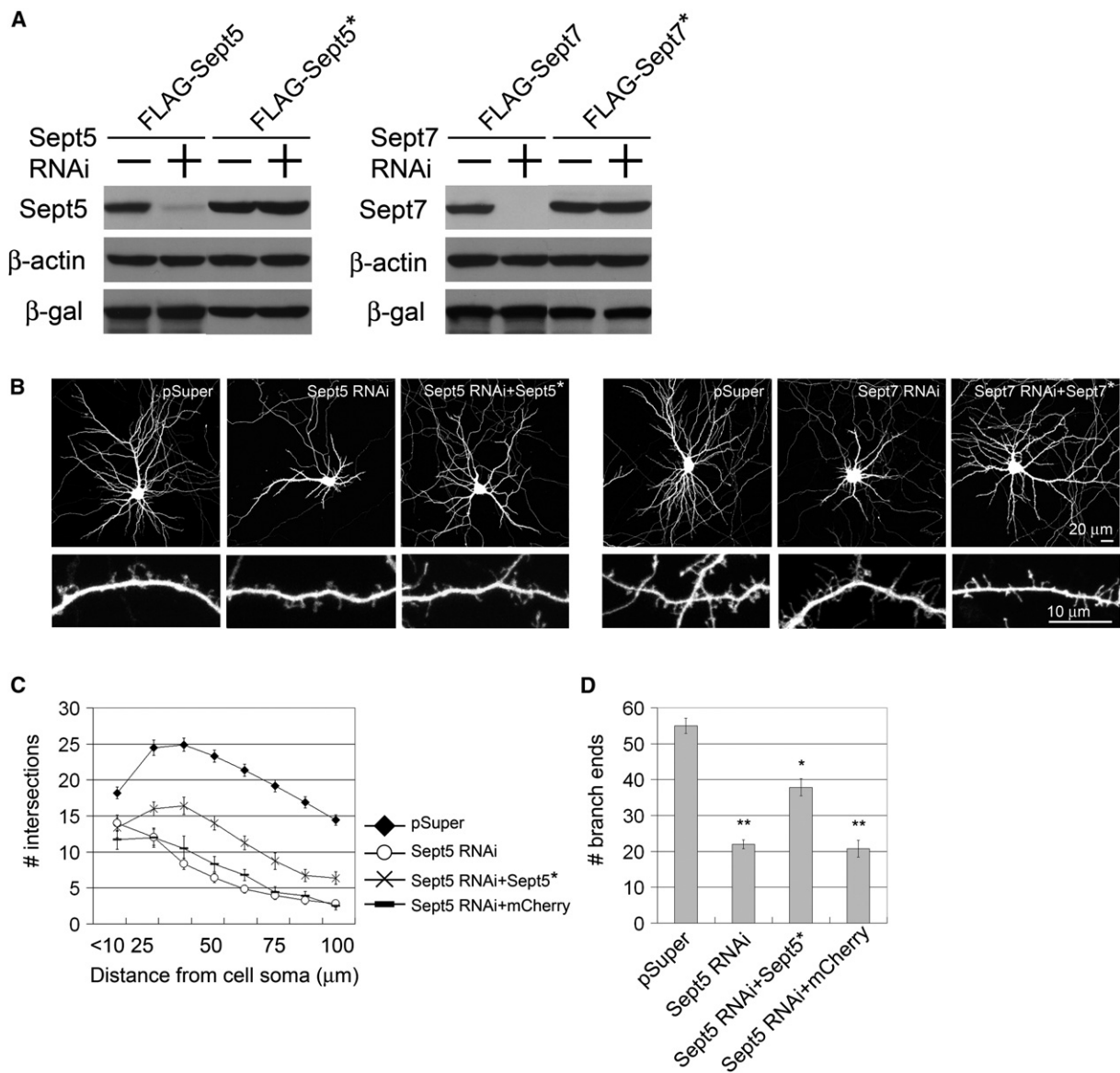


Figure S3. RNAi-Resistant Sept5 or Sept7 cDNAs and Rescue of Effect of RNAi against Sept5 or Sept7, Respectively

(A) HEK293 cells were transfected with Sept5, RNAi-resistant Sept5 (Sept5*), Sept7, or RNAi-resistant Sept7 (Sept7*) (all FLAG-tagged) together with pSuper vector control (-) or with pSuper-based RNAi constructs designed to knock down the specific septin indicated (+). Two days after transfection, FLAG-Septin levels were analyzed by immunoblotting with an anti-FLAG antibody. Sept5 and Sept7 RNAi constructs knock down expression of Sept5 and Sept7, respectively, but had no effect on the corresponding RNAi-resistant septin. β -actin was immunoblotted as a loading control and β -gal as a transfection control.

(B) Cultured hippocampal neurons (DIV7) were transfected with empty vector pSuper or Sept5 RNAi, Sept5 RNAi + Sept5*, Sept7 RNAi, or Sept7 RNAi+Sept7*, as indicated. At 5 days after transfection (DIV7+5), neuron morphology was visualized by immunostaining for cotransfected β -gal.

(C and D) Sholl analysis of dendrite branching (C) and branch-end counts (D), as shown in Figure 3. Cultured hippocampal neurons (DIV7) were transfected with empty vector pSuper, Sept5 RNAi, Sept5 RNAi+Sept5*, or Sept5 RNAi+mCherry, as indicated. Histograms show mean \pm SEM; ** $p < 0.01$, * $p < 0.05$, one-way ANOVA. "n" numbers for each condition were control pSuper (76), Sept5 RNAi (26), Sept5 RNAi+Sept5* (30), and Sept5 RNAi+mCherry (30).

Table S1. Plasmids Used in This Study

Plasmid	Promoter	Reference
pFLAG-CMV-2	CMV	Sigma-Aldrich Biotechnology
pFLAG-CMV-Sept2	CMV	Constructed by Makoto Kinoshita
pFLAG-CMV-Sept6	CMV	Constructed by Makoto Kinoshita
pFLAG-CMV-Sept7	CMV	Constructed by Makoto Kinoshita
pFLAG-CMV-Sept5*	CMV	This work
pFLAG-CMV-Sept7*	CMV	This work
pFLAG-CMV-mCherry	CMV	This work
pSuper	H1	Oligoengine
pSuper-ZnT3 shRNA	H1	[S1]
pSuper-EGFP shRNA	H1	Gift from Jacek Jaworski
pSuper-Sept2 shRNA	H1	This work
pSuper-Sept5 shRNA	H1	This work
pSuper-Sept6 shRNA	H1	This work
pSuper-Sept7 shRNA	H1	This work
pCMV-βgal	CMV	[S1, S2]
pβa-EGFP	chicken β-actin	[S2, S3]
pβa-EGFP-Sept2	chicken β-actin	This work
pβa-EGFP-Sept5	chicken β-actin	This work
pβa-EGFP-Sept6	chicken β-actin	This work
pβa-EGFP-Sept7	chicken β-actin	This work

Rattus norvegicus Sept2, Sept5, Sept6, and Sept7 were cloned from Rat Brain Matchmaker cDNA Library (Clontech) by PCR with two specific primers with appropriate restriction sites. We generated pβa-EGFP-Sept2, -Sept6, and -Sept7 by inserting respectively the Sept2, Sept6, and Sept7 PCR product into the BamHI and SpeI sites in a modified pβa-EGFP plasmid. We generated pβa-EGFP-Sept5 by inserting the Sept5 PCR product into the EcoRI and SpeI sites in a modified pβa-EGFP plasmid. RNAi-resistant cDNAs Sept5* and Sept7* were generated by site-directed mutagenesis, with no change in amino acid sequence of the corresponding protein. Modified sequence of RNAi-resistant Sept5 was 5'-TAGGAAACAAGTAGAAGA-3', and RNAi resistant Sept7, 5'-AGCCGACGACAAAACGACG-3' (in which the underlined nucleotide indicates a substitution from the endogenous rat cDNA sequence; compare to Table S2).

Table S2. RNAi Sequences Used in This Study

Plasmid	Sequence	Reference (GenBank Accession Number)
pSuper	Empty	Oligoengine
pSuper-ZnT3 shRNA	5'-GGGCATGGATACCCAATGT-3'	[S1]
pSuper-EGFP shRNA	5'-GCAAAGACCCCAACGAGAA-3'	Gift from Jacek Jaworski
pSuper-Sept2 shRNA	5'-CCAAGACCTTCACTATGAA-3'	Rat Sept2 (NM_057148)
pSuper-Sept5 shRNA	5'-AGAAGATGAAGCAGCGAAT-3'	Rat Sept5 (AB_027143)
pSuper-Sept6 shRNA	5'-GTGAAGATAGGAACAAGA-3'	Rat Sept6 (XM_001062917)
pSuper-Sept7 shRNA	5'-GCAACAGAATTCTTCAAGA-3'	Rat Sept7 (NM_022616)

The complementary oligonucleotides were annealed and inserted into the pSuper vector (Oligoengine).

Table S3. Production of Anti-Septin Antibodies

Target Septin	Antigen	Host Animal	Reference
Sept2	MSKQQPTQFINPETPGYV+C* of mouse Sept2	Rabbit	[S4]
Sept4	C*+CMLHKIQRQMKETH of mouse Sept4	Rabbit	[S5]
Sept5	C*+MLQRMKQQMQDQ of mouse Sept5	Guinea pig	[S6]
Sept6	C*+GGSQTLKRDKEKKN of mouse Sept6	Rabbit	Generated by Makoto Kinoshita
Sept7	C*+EQQNSSRTLEKNKKKGKIF of mouse Sept7	Guinea pig	[S6]
Sept11	C*+GVQIYQFPTDEETVAEI of mouse Sept11	Rabbit	Generated by Makoto Kinoshita

* A cysteine residue is added for the conjugation to BSA or KLH.